Preliminary Measurements of a Magnetic Steering System for RF Plasma Thruster Applications

Antonella Caldarelli*
Te Pūnaha Ātea - Auckland Space Institute, The University of Auckland, Auckland, New Zealand, 1010

Félicien Filleul†
Te Pūnaha Ātea - Auckland Space Institute, The University of Auckland, Auckland, New Zealand, 1010

Christine Charles‡
Space Plasma, Power and Propulsion Laboratory, Australian National University, Canberra, Australia, 2601

Nicholas Rattenbury § and John Cater¶
Te Pūnaha Ātea - Auckland Space Institute, The University of Auckland, Auckland, New Zealand, 1010

Preliminary measurements of a magnetic thrust vectoring (MTV) system to be implemented in a magnetic nozzle RF plasma thruster are presented. The system comprises two coaxial coils capable of generating magnetic nozzle deflections of 15° with respect to the system axis. The MTV system is numerically modelled to compute the magnetic field vector. The experiments are carried out in Huia, a RF plasma reactor dedicated to the study of magnetic nozzle electrode-less plasma thrusters at the University of Auckland. The ion saturation current is mapped in the plasma source using a Langmuir probe for two cases: 1) the magnetic nozzle is axisymmetrical, and 2) the magnetic nozzle is deflected. Spatial measurements show an increase in ion saturation current in the radial direction following the magnetic field gradient, and the plasma profile seems to trail the magnetic field streamlines in the region of ion magnetisation. Validation of plasma potential measurements obtained from a retarding field energy analyser is also presented.

Nomenclature

B_z	=	Magnitude of magnetic field on axis
I_{sat}	=	Ion saturation density
n_p	=	Plasma density
$r_{g,i}$	=	Ion gyroradius
T_e	=	Electron temperature
V_C	=	Collector grid voltage
V_D	=	Discriminator grid voltage
V_p	=	Plasma potential
α	=	Angle between the coil axis and the system axis z
θ_{def}	=	Deflection angle of the central magnetic field line with respect to the system axis z

I. Introduction

Controlling the attitude of a spacecraft can be achieved through controlling the direction of the thrust vector. Attitude and orbit control (AOC) has previously been accomplished using mechanically actuated gimbal platforms, momentum

*PhD Student, Department of Engineering Science, acal877@aucklanduni.ac.nz.
†PhD Student, Department of Physics, ffli056@aucklanduni.ac.nz.
‡Professor, Centre for Plasmas and Fluids, Research School of Physics, christine.charles@anu.edu.au, AIAA Senior Member.
§Senior Lecturer, Department of Physics, n.rattenbury@auckland.ac.nz.
¶Associate Professor, Department of Engineering Science, j.cater@auckland.ac.nz, AIAA Life Member.

wheels or, for larger spacecraft, vernier thrusters [1]. Mechanical systems are usually heavy and complex and like any other moving equipment they are delicate pieces of hardware which add potential failure modes to the mission. The concept of magnetic thrust vectoring, however, relies on a steerable magnetic nozzle (MN) to control the direction of a plasma beam, and no moving components are required. The lack of electrodes and neutralisers, together with the advantage of the magnetic nozzle in reducing plasma cross-field diffusion, could increase the lifetime of the propulsion system, making radio-frequency (RF) electrode-less plasma thrusters a competitive choice for future low-thrust space missions. With a view to developing plasma propulsion systems that can be used in small- and nano-satellites, magnetic thrust vectoring would allow for a simpler and more reliable orbit and attitude control mechanism.

Burkhart and Seikel [2] were the first to present the idea of using a magnetic field to control the direction of the thrust vector generated by an electric propulsion system. In a low-power magnetoplasmadynamic (MPD) thruster, they recorded a deflection of the ion exhaust beam flux of up to ±5°, resulting from a shift of up to ±5° in the axis of the magnetic field. However, the magnetic steering experiment was restricted to one direction.

Cox et al. [3] carried out experimental studies on steering a plasma beam in the RF helicon plasma reactor Chi-Kung at the Australian National University (ANU) by using transverse magnetic fields (TMF). It was noticed that the ion beam was effectively deflected as a result of the TMF, and that the angle of plasma deflection increased as the magnetic field was deflected further. It was also reported that the magnetic field was not the dominant factor in controlling ion beam deflection and that the plasma behaviour was different for different solenoid polarities. However, the causes of such plasma behaviour were not investigated and the magnetic steering was constrained in one plane.

Merino and Ahedo [4] proposed a low-power 3D magnetic thrust vectoring (MTV) system made of coaxial coils that could be used for plasma propulsion applications. This thrust vectoring system does not require any moving structures as the plasma deflection is accomplished by controlling the orientation of the magnetic nozzle. However, the concept has only been shown to work in numerical simulations and the plasma was assumed to be fully ionised and magnetised.

The purpose of this research is to present a preliminary investigation of a magnetic steering system for RF plasma thruster applications based on the study carried by Merino and Ahedo [4]. This is accomplished, in the initial phase, through the testing of a non-axisymmetric magnetic field incorporated into Huia, a new experimental apparatus dedicated to the study of the physical principles of magnetic nozzle radio-frequency plasma thrusters at the University of Auckland. The assessment of the ion saturation current profile inside the source allows the detection of changes in the plasma spatial mapping when the magnetic nozzle is deflected. The plasma generation is obtained using Huia's main axial coils and the MTV system is used to test the steering of the flowing plasma. Preliminary results of plasma deflections in 2D measured using a Langmuir probe are presented. Additionally, validation of a retarding field energy analyser (RFEA) is done, and the Ion Energy Distribution Function (IEDF) and plasma potential, V_p, are measured.

The paper is organised as follows. The magnetic vectoring system is described and the achievable magnetic field deflections are presented is Section II. In Section III the experimental apparatus and the plasma diagnostics are described. Lastly, Sections IV and V discuss the spatial measurements of the ion saturation current and plasma potential measurements.

II. Two-Dimensional Magnetic Vectoring System

The preliminary design of the magnetic thrust vectoring (MTV) system used to steer an expanding plasma in a electrode-less RF plasma reactor includes a copper coil mounted coaxially with the plasma source, but inclined at an angle $\alpha = 15°$ with respect to the source axis. These two magnets form the 2D MTV system and the assembly is shown in Figure 1. The deflection of the magnetic nozzle on the r-z plane is accomplished by using the MTV system to steer the divergent part of a symmetric magnetic nozzle created by a second set of coils, here defined as 'main coils'. The centre of the steering coils is placed at (r, z) = (0 cm, 23 cm), while the main coils are located so that their middle point coincides with the antenna centre (r, z) = (0 cm, 0 cm).

The MTV system is modelled using ANSYS Electronics Desktop 2021-R1 to compute the magnetic field topology in the plasma source. The simulations are run using the software's 3D Magnestotatic solver which computes Maxwell's equations via the Finite Element Method [5]. A validation of the ANSYS model was conducted to ensure that the magnetic field calculated by the software solver yielded accurate results. Measurements of $\vec{B}$ along the axis are carried out using a DTM-133 digital Teslameter and an MPT-132 Hall probe by Group3, and the simulated and measured data show an agreement within ±2%.

Figures 2a and 2b show the simulated magnetic field lines and contour plots inside the plasma source for cases: 1) the MTV system is placed at $\alpha = 0°$, thus no MN deflection is present, and 2) the MTV system is rotated by $\alpha = 15°$. The resulting $\vec{B}$ exhibits a single peak along the z-axis extending into a diverging field which decreases rapidly after the

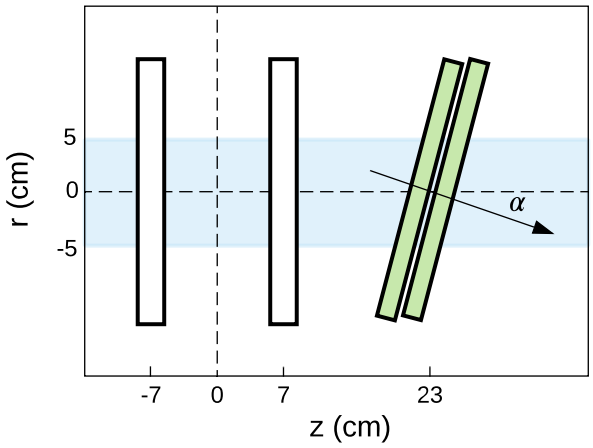

Fig. 1 Coils assembly on Huia. In white, the 'main coils', while in green are the two coils that form the 2D magnetic vectoring system. The centre of the antenna is at (r, z) = (0 cm, 0 cm). α is the angle between the plasma source axis and the 2D MTV system axis z. The MTV coils are placed 23 cm from the antenna centre due to space constraints in the set up. In blue, the plasma source tube.

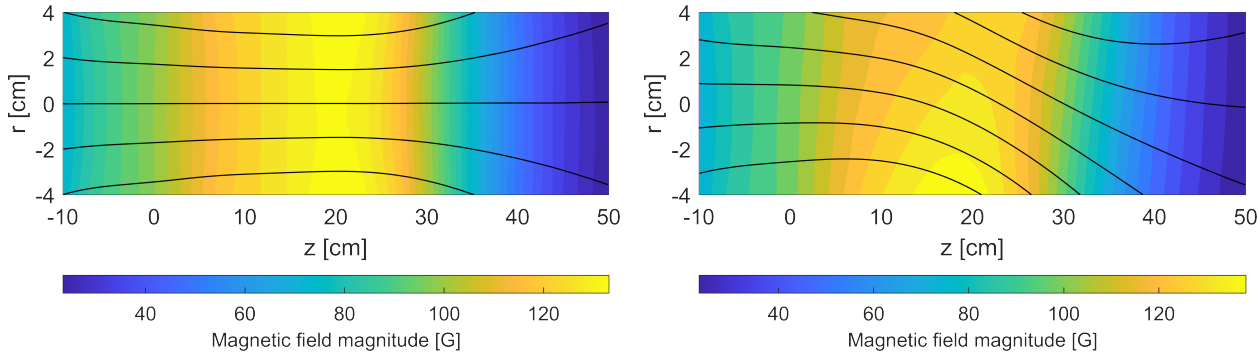

Fig. 2 Contour plots of the magnitude of the magnetic field together with the field lines (black lines) for (a) $\alpha = 0°$ and (b) $\alpha = 15°$. The aspect ratio of the plots is set to [0.4, 1] for visual clarity.

throat point, i.e. (r, z) = (0 cm, 23 cm), for both case 1 and 2. The magnitude of the magnetic field on axis (r = 0 cm), B_z, for the two different configurations is calculated to remain almost unchanged and a peak magnetic field $B_{z,max}$ of 135 G is achieved close to the throat location when the main coils and the MTV coils are powered at 3 A and 20 A, respectively. Deflections of the centre streamline of the magnetic nozzle, θ_{def}, of 15° are predicted on the r-z plane from magnetostatics simulations - shown in Fig. 2b.

It is noted that in this configuration θ_{def} is constrained to 15°. Indeed, the effective deflection angle θ_{def} of the magnetic nozzle is constrained by the choice of α; this also means that the $\vec{B}$ field will not be deflected by more than α independently of how much the 'critical' current value, I_{min}, is increased. For instance, the minimum current necessary to obtain a $\theta_{def} \approx 15°$ is I_{min} = 10 A, when the current in the 'main coils' is set at 3 A. However, the achievable MN orientation would be sufficient to perform attitude and orbit control manoeuvres for spacecraft as the majority of thrust vectoring corrections do not exceed 15°.

A. Plasma Magnetisation

The effective deflection of the plasma achieved by controlling the orientation of the magnetic nozzle depends mainly on the coupling between the plasma and the magnetic field. A preliminary method to classify this relationship

is by analysing the magnetisation of the ions. In the ideal case in which the ion population is fully magnetised, the plasma plume deflection would correspond to the MN deflection since the ions would follow to the field lines. Full ion magnetisation is characterised by $r_{g,i} << L$, where $r_{g,i}$ is the ion gyroradius and L is the characteristic length of the system.

In reality, the ions in a RF plasma source are fully magnetised only in the near-region plume for strong enough magnetic fields, and ion magnetisation decreases along the nozzle axis. A preliminary analysis of the ion gyroradius along the axis is done to estimate the plasma behaviour with the deflecting magnetic nozzle for case 2. Figure 3 compares $r_{g,i}$ with the normalised magnetic field strength, both calculated along the axis and assuming an ion thermal speed of 400 m/s [6]. In the region of highest magnetic field strength, the ion gyroradii are expected to be smaller than L, where the radius of the plasma source was considered to be the characteristic length of the system. From these results, fully magnetised ions can be expected in the near-region of the deflected magnetic nozzle.

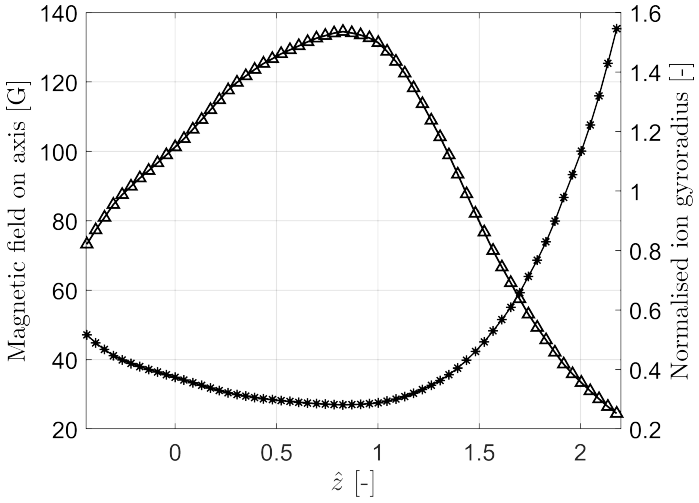

Fig. 3 Comparison of the normalised ion gyroradius (right axis, asterisks) and the magnetic field (left axis, triangles) along the system axis z. The axial position z is normalised with respect to the MN throat location, i.e. (r, z) = (0 cm, 23 cm). The gyroradius is normalised with respect to the plasma source radius.

III. Experimental Apparatus

Preliminary testing of a 2D magnetic steering system is conducted in the apparatus shown in Fig. 4. The experimental set up comprises the RF plasma reactor Huia, the 2D magnetic thrust vectoring system, and the plasma diagnostic system. Huia is a new variation of Echidna, a linear plasma device at ANU [6]. It is based on a 300 mm long steel chamber extended by a 1500 mm long, 90 mm inner diameter glass tube, pumped down to a base pressure $< 10^{-6}$ Torr. The plasma is created by a 190 mm long double-saddle antenna matched via an L-type matching network to maximise power transfer from a variable frequency (25-42 MHz) 1 kW generator. An axial magnetic field is applied by a pair of solenoids (denoted as main coils). Their inter-spacing and position along the z axis of Huia can both be varied to produce a wide range of magnetic field configurations. When in Helmholtz configuration, they provide a maximum axial magnetic field strength of ~ 23.81 G/A. During the experiments, the flow rate of argon is maintained at 10 sccm by the use of a mass flow controller to maintain a pressure of 1 mTorr.

Due to the limited volume of the glass tube, the formation of an ion beam is hindered, and plasma deflections are limited. Thus, this study aims to provide an initial evaluation of the plasma behaviour in a non-axial magnetic nozzle. In order to generate an ion beam, and the steering of the latter, an expansion chamber is required. Henceforth, the next phase of the study will expand Huia with a cylindrical stainless steel vacuum chamber (500 mm diameter, 700 mm long) where the plasma expansion in a magnetic nozzle deflected in 3D will be analysed.

A. Plasma Diagnostics

Two dimensional (r,z) mapping of the ion saturation current I_{sat} in Huia is used to detect steering of the plasma within the region of the deflected MN. The measurements are obtained with a Langmuir probe made out of a single

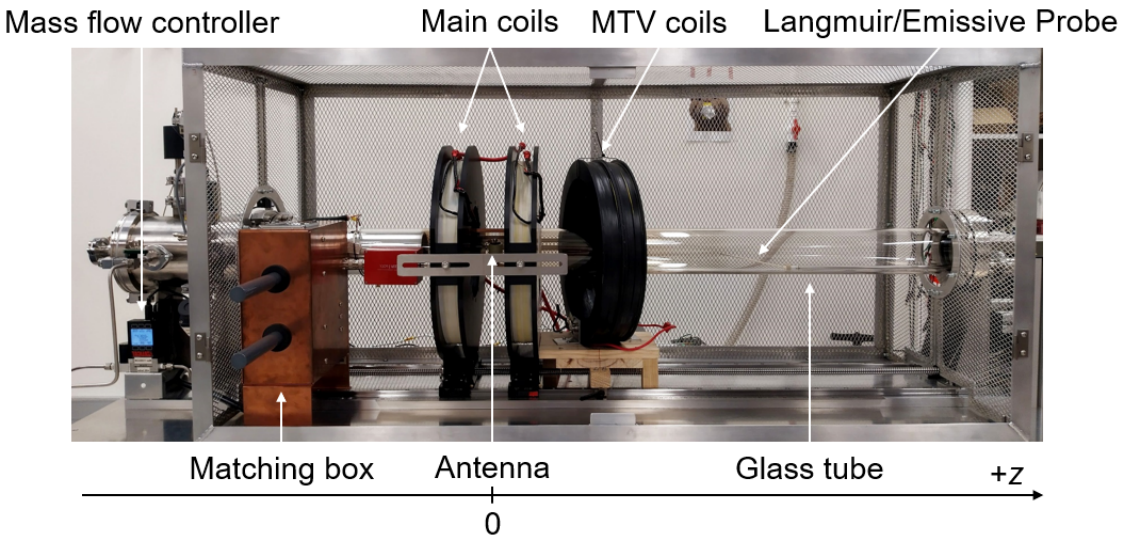

Fig. 4 Experimental apparatus Huia showing the two MTV coils in black. The LP and EP are inserted into the tube from the right hand side. The RFEA is inserted from the left.

sided 2 mm diameter nickel disk biased at -100 V to ensure total electron rejection. The probe is mounted on a 3 mm diameter ceramic tube attached to a movable (rotation and translation) shaft introduced in the downstream end of Huia and resting at the bottom of the glass tube. The shaft is covered with a 10 mm outer diameter glass sheath in order to minimise the disturbance to the dielectric boundary condition inherent to Huia. The ion saturation current is used instead of the plasma density n_p as a qualitative evaluation of the plasma deflection since n_p requires the knowledge of the spatial distribution of electron temperature T_e. The latter was reported to be spatially varying in a plasma reactor operating under similar conditions [6]. As accurate spatial measurements of T_e are beyond the scope of this study, only the ion saturation current is reported.

The validation of a retarding field energy analyser probe is carried out. The RFEA is used in ion collection mode to obtain the Ion Energy Distribution Function and the plasma potential. Given the significant size of the RFEA head (3.5cm x 2cm) with respect to the glass tube, the plasma is perturbed and measurements may be affected due to the increased rate of ion loss to the grounded RFEA head and shaft and by probable induced shifts in local plasma potentials. Consequently, the RFEA is only presently used for calibration procedures and is kept fixed at z = -12 cm so that the deflection of the plasma is not disturbed by the probe. The RFEA will be used in the subsequent part of the project to detect the presence and deflection of an ion beam in an expansion chamber.

The design of the RFEA is based on [7], whose similar design was also used in [8–10]. The probe head, shown on the top right corner of Fig. 5, has an orifice diameter of 2 mm and is connected to a 1 m long shaft via a Swagelok® fitting. Figure 5 shows a schematic of the analyser circuit. The first grid is earthed (E). The repeller grid (R), biased to -100 V by a DC high voltage power supply, repels the electrons entering the probe. The voltage of the discriminator grid (D) is swept from 0 to 80 V by a bipolar power supply. The role of the discriminator is to regulate the ions entering the analyser: for example, when the bias voltage is set to 50 V, only ions with an energy greater than this can pass through the RFEA and their current be collected. The secondary grid (S) is biased to -18 V and its role is to suppress the formation of secondary electrons caused by ion impact on the collector plate. The collector plate (C) is biased to -9 V. Both the secondary grid and the collector plate are biased via two batteries internal to the RFEA external electronics box. The current acquisition is done through electronics connected to a data acquisition (DAQ) system. A MATLAB® code controls the operation of the RFEA: it sets the biasing of the discriminator grid, reads and processes the data collected by the DAQ unit. The electronic boxes are wired to the plasma probe grids through a vacuum-tight circular push-pull connector with four wire terminals.

An emissive probe (EP) is used to measure the plasma potential at the same conditions and location as the RFEA in order to check the validity of the RFEA data. The EP is made out of a 0.127 mm U-shaped tungsten filament placed at the end of a 2 mm diameter two bores ceramic tube which is mounted on the same glass shaft used for the Langmuir probe. The floating potential method is used to determine the local plasma potential; an increasing heating current is flown through the filament in order to warm it up to thermionic emission as the floating potential of the filament

is synchronously recorded to produce a voltage-current curve. As the electron emission increases, it progressively neutralises the sheath around the filament. This corresponds to a sharp increase of the filament floating potential up to an inflection point at V_p, when the bulk of the electron distribution are recollected by the EP.

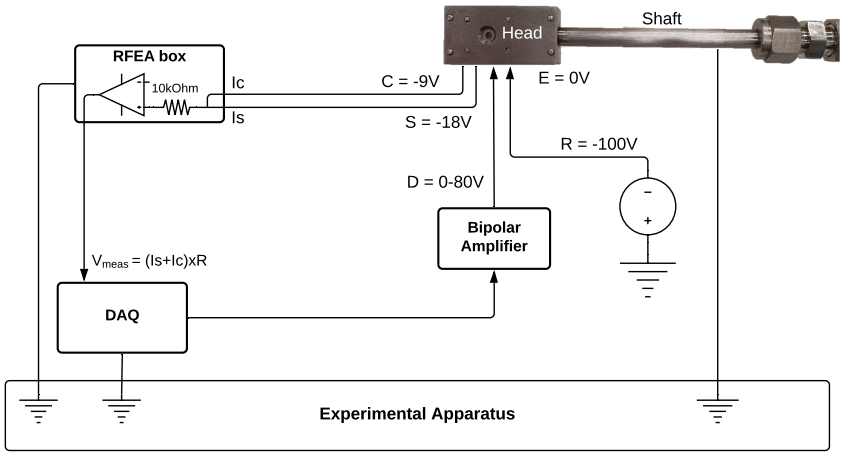

Fig. 5 Schematic of the RFEA circuit including a picture of the analyser head and support used in Huia. The probe orifice diameter is 2mm. The circuit shows the earth E (0 V), repeller R (-100 V), discriminator D (0 - 80 V), secondary S (-18 V) and collector C (-9 V) voltages. The signal measured by the RFEA is the sum of the secondary and collector currents. This current flows through a 10 kΩ resistor to ground, where the voltage is calculated after passing through a buffer amplifier. The gain of the buffer amplifier can be adjusted through a switch on the RFEA circuit.

IV. Spatial Ion Saturation Measurements

Measurements in this section focus on identifying asymmetries in the plasma density profile as a result of the deflected MN. Firstly, spatial measurements of the ion saturation current are performed when $\alpha = 0°$ to obtain a baseline profile to compare with measurements made when the MTV coils are rotated of 15°. The Langmuir probe is moved along the z-axis in the region $-10 < z < 50$ cm and is swept radially between $-4 < r < 4$ cm. Measurements are carried out in an argon plasma operating at 300 W, at a frequency of 27.12 MHz, with $B_{z,max}$ of 135 G and at a nominal pressure of 1 mTorr. The sampling rate is set to 1×10^5 samples/s and the average standard deviation of the measurements is 8 μA

Figure 6a and 6b show the contour plots of the recorded I_{sat} and the calculated magnetic field lines for $\alpha = 0°$ and $\alpha = 15°$, respectively. For the case in which the MTV coils are not rotated (case 1), the plasma presents a peak of ion saturation current in the region of $-10 < z < 23$ cm and $-1.5 < r < 1.5$ cm. After the MN throat, I_{sat} drops following the decrease in B_z. This is an expected behaviour: I_{sat} peaks in the region under the antenna ($-10 < z < 10$ cm), and where the magnetic field strength is higher (i.e. $10 < z < 23$ cm) and the plasma is radially constrained by the magnetic streamlines. It has to be noted that due to the symmetrical nature of case 1, the data is collected only in half of the source and then mirrored as the plasma is assumed to be symmetrical with respect to the axis z.

On the other hand, when $\alpha = 15°$, the ion saturation current peaks in the region of $-10 < z < 10$ cm and $-2 < r < 2$ cm. The drop in I_{sat} between $10 < z < 23$ cm is probably due to the increased plasma flux to the radial walls following the bent field lines. Indeed, as the magnetic field shows a fairly uniform configuration in the region under the antenna, the magnetic field deflects significantly at $z > 10$ cm. Analysing the 2D profile of I_{sat}, it presents clear asymmetries. It can be observed in Fig. 6b that the plasma bulk seems to follow the magnetic streamlines. The ion saturation current increases in the negative radial direction where the magnitude of the magnetic field is higher, as seen is Fig. 2b. However, for $z > 30$ the ion density profile is fairly symmetrical; in that region, the strength of the magnetic field is not high enough to keep the ions magnetised. Table 1 summarises three data sets of I_{sat}, where each data set is measured at the same axial location but opposite radial coordinate.

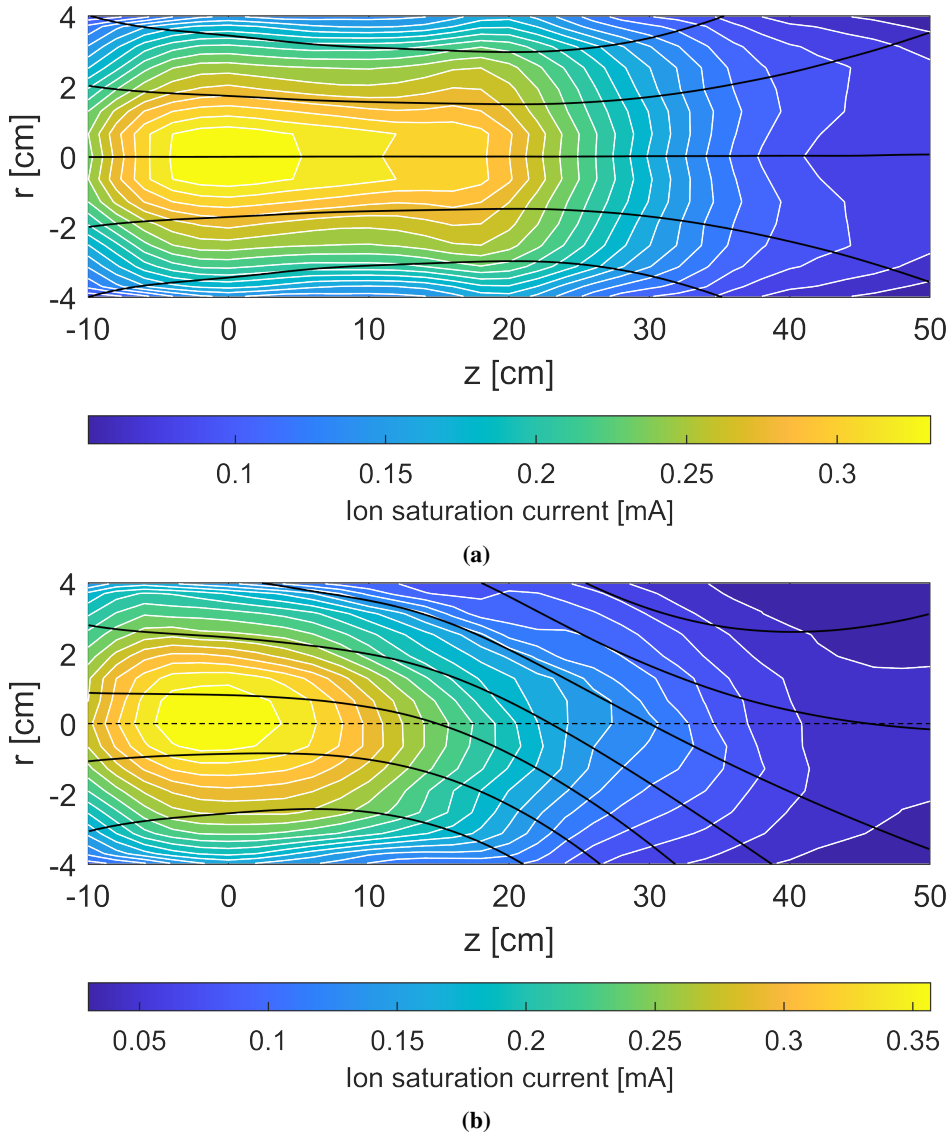

Fig. 6 Contour plots of the ion saturation current for (a) $\alpha = 0°$ and (b) $\alpha = 15°$. Black lines are the magnetic field lines. The aspect ratio of the plot is set to [0.4, 1] for visual clarity.

Table 1 Ion Saturation Current Measured at Six Different Locations

z [cm]	r [cm]	I_{sat} [mA]
10	-2.5	0.25
	+2.5	0.21
20	-2.5	0.17
	+2.5	0.12
30	-2.5	0.10
	+2.5	0.09

V. Plasma Potential Measurements

As mentioned in Section III, the size of the RFEA with respect to the glass tube cross-sectional area would cause significant plasma perturbations. Thus, spatial measurements of the IEDF are not carried out in Huia as the plasma profile could be affected. Instead, only the validation of the retarding field energy analyser is done in the plasma source.

The potential of Argon plasma is measured at RF powers of 150 W, frequency of 27.12 MHz, 1 mTorr, 470 G peak $|\vec{B}|$, and the probe orifice is kept fixed at (r_{RFEA}, z_{RFEA}) = (0 cm, -13 cm). For V_{p} measurements in Huia, only the 'main coil' are used and, unless specified otherwise, their centre position is at (r, z) = (0 cm, 0 cm).

The measurements are done by sweeping $\mathrm{V_D}$ from 0 to 80V in 300 steps; at each discriminator voltage, 200 readings of the collector voltage are performed and subsequently averaged. To calculate the derivative of $\mathrm{V_C(V_D)}$, a Savitzky-Golay (SG) filter is applied to the data (shown in Fig. 7a) which is then numerically differentiated to obtain the IEDF. An SG filter is also applied to the raw IEDF to smooth the noise introduced by the derivative operation. The negative of the IEDF shows a Gaussian peak around the same $\mathrm{V_D}$ range of the sharp decrease in the collector voltage. This peak corresponds to the local plasma potential and is equal to 56.6 ± 1 V for the analysed case, as seen in Fig. 7b. The EP is subsequently placed at (r, z) = (0 cm, -13 cm) under the same plasma conditions and recorded a plasma potential of 55.1±3 V.

Comparison between the V_{p} measured by the RFEA and the emissive probe is also done at: 1) 180 W, 1 mTorr, $B_{\mathrm{z,max}}$ = 470 G, and (r_{RFEA}, z_{RFEA}) = (0 cm, -13 cm); and 2) 200 W, 1 mTorr, $B_{\mathrm{z,max}}$ = 300 G, (r_{RFEA}, z_{RFEA}) = (0 cm, -10 cm), and the 'main coils' are moved to (r, z) = (0 cm, 30 cm). Table 2 summarises the plasma potentials measured by the field analyser and the EP taken at the different experimental conditions.

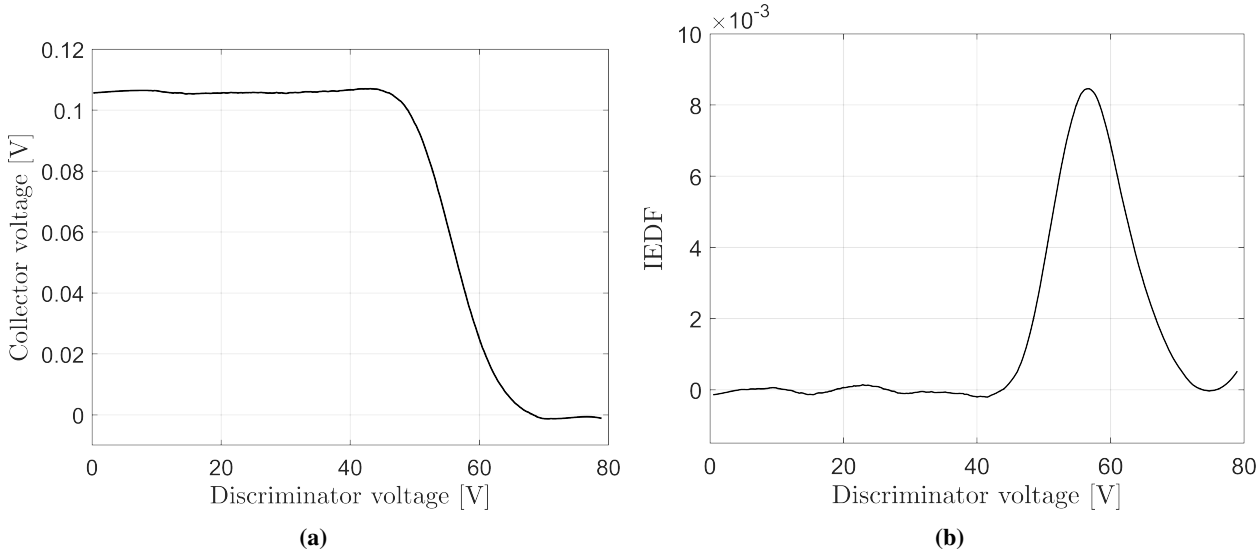

(a) **(b)**

Fig. 7 (a) Best-fit curve of the voltage measured at collector plate $\mathrm{V_C}$ against the discriminator grid voltage $\mathrm{V_D}$. The standard deviation of $\mathrm{V_C}$ was calculated to be 4 mV. (b) Best-fit Gaussian ion energy distribution function (IEDF) against discriminator grid voltage. The peak of the curve Gaussian shows a plasma potential of 56.6 V.

Table 2 Plasma Potential Measurements

Plasma conditions	Probe	V_{p} [V]
150 W, 1 mTorr, $B_{\mathrm{z,max}}$ = 470 G	RFEA	56.6
	EP	55.1
180 W, 1 mTorr, $B_{\mathrm{z,max}}$ = 470 G	RFEA	58.2
	EP	57.2
200 W, 1 mTorr, $B_{\mathrm{z,max}}$ = 300 G	RFEA	37.7
	EP	38.1

VI. Conclusions

A preliminary investigation of a magnetic thrust vectoring system was carried out. The study is conducted in a new RF plasma reactor, Huia, at the University of Auckland. Magnetic nozzle deflections of up to 15° were expected from magnetostatic simulations.

Spatial measurements of the ion saturation current in the plasma source made with an LP showed that for case 2 (i.e. where the MTV coils are rotated by 15°) the plasma profile presents asymmetries on the r-z plane and, as expected, the increase in ion saturation current follows the radial gradient of the magnetic field strength in the region of ion magnetisation. A comparison between the spatial measurements of I_{sat} and the magnetic field lines shows that the plasma profile trails the magnetic field lines. Thus, from the collected data it is inferred that the plasma is being deflected as a consequence of the non-symmetrical magnetic nozzle.

A validation of the RFEA was also done. In the analysed case (RF power of 150 W, $B_{\text{z,max}}$ of 470 G and 1 mTorr) a V_{p} of 56.6 ± 1 V is measured. The value agrees well with data collected by an emissive probe at the same plasma conditions and location. The comparison between plasma potentials measured by the RFEA and the EP at different experimental conditions also shows a good agreement between the two probes.

The limitations of this study are mainly due to the restricted plasma source cross-sectional area that leads to a: 1) a restrained plasma deflection, as plasma losses to the tube walls incur fast, and 2) a hindered ion beam formation, which presence is crucial for an efficient thrust generation in propulsion applications. The analysis is also limited in 2D. The next stage of the research involves the testing of an MTV system capable of steering the plasma in 3D, and the study of an ion beam expansion and generation in a deflected magnetic nozzle.

Acknowledgements

This research is being funded by the Asian Office of Aerospace Research and Development (AOARD), the international office of the Air Force Office of Scientific Research (AFOSR).

References

[1] Sutton, P. G., and Biblarz, O., *Rocket Propulsion Elements*, ninth ed., John Wiley and Sons, Inc., New York, 2017, Chap. 18, pp. 671–689.

[2] Burkhart, J. A., and Seikel, G. R., "Feasibility Studies on an Auxiliary Propulsion System Using MPD Thrusters," *Journal of Spacecraft and Rockets*, Vol. 9, No. 7, 1972, pp. 487–488.

[3] Cox, W., Charles, C., Boswell, R. W., Laine, R., and Perren, M., "Magnetic Ion Beam Deflection in the Helicon Double-Layer Thruster," *Journal of Propulsion and Power*, Vol. 26, No. 5, 2010, pp. 1045–1052.

[4] Merino, M., and Ahedo, E., "Contactless steering of a plasma jet with a 3D magnetic nozzle," *Plasma Sources Science and Technology*, Vol. 26, 2017, p. 095001.

[5] ANSYS Inc., "ANSYS Maxwell V16 Training Manual," , 05 2013. URL `https://docplayer.net/35134651-Ansys-maxwell-v16-training-manual.html`, rev. 14.5.

[6] Bennet, A., Charles, C., and Boswell, R., "Non-local plasma generation in a magnetic nozzle," *Physics of Plasmas*, Vol. 26, No. 7, 2019, p. 072107.

[7] Conway, G. D., Perry, A. J., and Boswell, R. W., "Evolution of ion and electron energy distributions in pulsed helicon plasma discharges," *Plasma Sources Science and Technology*, Vol. 7, No. 3, 1998, pp. 337–347.

[8] Cox, W., "Magnetic Steering of the Ion Beam in the Helicon Double Layer Thruster," Ph.D. thesis, Australian National University, 2010.

[9] Lafleur, T. A., "Helicon Wave Propagation in Low Diverging Magnetic Field," Ph.D. thesis, Australian National University, 2011.

[10] Bennet, A., "Low Pressure Plasmas in Magnetic Nozzles," Ph.D. thesis, Australian National University, 2019.